Supporting Information for:

Rock-salt-type nanoprecipitates lead to high thermoelectric performance in undoped polycrystalline SnSe

Guodong Tang,[1,*] Qiang Wen,[1] Teng Yang,[2,*] Yang Cao,[1] Wei Wei,[1] Zhihe Wang,[3,*] Zhidong Zhang,[2] Yusheng Li[1]

[1]Department of Materials Science and Engineering, Nanjing University of Science and Technology, Nanjing 210094, China.

[2]Shenyang National Laboratory for Materials Science, Institute of Metal Research, Chinese Academy of Sciences, 72 Wenhua Road, Shenyang 110016, China.

[3]National Laboratory of Solid State Microstructures, Department of Physics, Nanjing University, Nanjing 210093, China.

Corresponding authors:

*tangguodong@njust.edu.cn (G.T.); yangteng@imr.ac.cn (T.Y.); zhwang@nju.edu.cn (Z.W.).

Content:

Boltzmann transport calculations

The band structures of SnSe were calculated using the general potential linearized augmented plane-wave (LAPW) method as implemented in the WIEN2K package.[32] The electronic exchange–correlation was described within the generalized gradient approximation (GGA) of Perdew–Burke–Ernzerhof (PBE) flavor.[33] We used 5000 k points in the full Brillouin zone (BZ) to achieve a total energy convergence better than 1 meV/atom. The atomic structures of SnSe *Pnma* and $Fm\bar{3}m$ phases are shown in Figs. S2a and S2b, respectively. To compare the thermoelectric transport properties between pure phases of $Fm\bar{3}m$ cubic rocksalt and *Pnma* orthorhombic, we calculated the electrical conductivity σ, Seebeck coefficient *S*, and *PF* of two single phases as functions of temperature and carrier concentration *n* by using first-principles density functional theory and show the results in Fig. S5. The transport properties were obtained from the conductivity distributions

$$\sigma_{\alpha\beta}(T;\mu) = \frac{1}{\Omega}\int \sigma_{\alpha\beta}(\varepsilon)\left[-\frac{\partial f_{\mu}(T;\mu)}{\partial \varepsilon}\right]d\varepsilon \quad , \tag{2}$$

$$\kappa_{\alpha\beta}(T;\mu) = \frac{1}{e^2 T\Omega}\int \sigma_{\alpha\beta}(\varepsilon)(\varepsilon-\mu)^2\left[-\frac{\partial f_{\mu}(T;\mu)}{\partial \varepsilon}\right]d\varepsilon \quad , \tag{3}$$

$$S_{\alpha\beta}(T;\mu) = \frac{(\sigma^{-1})\gamma\alpha}{eT\Omega}\int \sigma_{\gamma\beta}(\varepsilon)(\varepsilon-\mu)\left[-\frac{\partial f_{\mu}(T;\mu)}{\partial \varepsilon}\right]d\varepsilon \quad , \tag{4}$$

where $\sigma_{\alpha\beta}$, $\kappa_{\alpha\beta}$, and $S_{\alpha\beta}$ are the electrical conductivity, electronic thermal conductivity and Seebeck coefficient, respectively. The energy projected conductivity tensor s_{ab} (e) can be defined as[34]

$$\sigma_{\alpha\beta}(\varepsilon) = \frac{1}{N}\sum_{i,k}\sigma_{\alpha\beta}(i,k)\frac{\delta(\varepsilon-\varepsilon_{i,k})}{d\varepsilon} \quad , \tag{5}$$

with

$$\sigma_{\alpha\beta}(i,k) = e^2\tau_{i,\kappa}v_\alpha(i,k)v_\beta(i,k), \qquad v_\alpha(i,k) = \frac{1}{\hbar}\frac{\partial\varepsilon_{i,k}}{\partial k_\alpha}, \tag{6}$$

where τ is the electronic relaxation time; group velocity v_α can be calculated from band structure $\varepsilon_{i,k}$. The electronic relaxation time τ was assumed to be independent of energy.[34-36]

We calculated the transport properties based on the Boltzmann transport theory applied to the band structure. No adjustable parameters were needed to calculate these transport functions. The integration with a very dense mesh of up to 18000 k points in the BZ was done within the BOLTZTRAP transport code.[36]

Our calculations show that *S* between *Pnma* and $Fm\bar{3}m$ phases does not evidently differ. Both types of carriers (electron and hole) yield a similar magnitude of *S* (Fig. S5a and S5d). In contrast, a considerable distinction between *Pnma* and $Fm\bar{3}m$ phases is found in terms of electrical conductivity and *PF*. A comparison of the band structures of $Fm\bar{3}m$ (Fig. S4) and *Pnma* phases reveals that the top valance band and the bottom conduction band of $Fm\bar{3}m$ phase show a much larger band dispersion (or smaller effective carrier mass) than that of the *Pnma* phase; as a result, the carrier mobility of $Fm\bar{3}m$ is higher than that of *Pnma*. Electrons may be advantageous over holes in the improvement of the electronic transport of SnSe (Fig. S5b and S5e). Fig. S5b and S5e further show that the doping effects on the $Fm\bar{3}m$ phase are much more pronounced than those on the *Pnma* phase under similar carrier concentration *n*. Using *n* (approximately 10^{-4} hole/unit cell) derived from Hall measurements, we calculated *PF* of $Fm\bar{3}m$ and *Pnma* phases (Fig. S5c and S5f; green dashed lines were used to highlight the

experimental doping levels of both phases). A higher *PF* was expected in the former than in the latter. The *PF* of $Fm\bar{3}m$ phase (Fig. S5c) in our experiment is at the brink of the area where a more pronounced *PF* is expected (Fig. 3c). A slightly higher hole carrier concentration (less than one order of magnitude) may substantially improve *PF* of $Fm\bar{3}m$. In contrast, Fig. S5f shows that the experimental *n* of the *Pnma* phase is far from the optimal area.

Table S1: The lattice parameters extracted from the XRD Rietveld refinement (Fig. S1) for two phases of SnSe (*Pnma* and $Fm\bar{3}m$).

SnSe	a (Å)	b(Å)	c (Å)
Pnma	11.51(5)	4.14(9)	4.45(5)
Fm-3m	5.89(7)		

Fig. S1. XRD pattern with Rietveld refinement for as-grown polycrystalline SnSe. All the peaks can be indexed with the cubic and orthorhombic phase of SnSe. Below the experimental data fitted by a red line, there are two rows of vertical blue bars and a green line. The green line represents the difference between the experimental XRD data and our Rietveld refinement data. The upper blue bars represent the peak positions for *Pnma* phase of SnSe, while the lower blue bars for cubic phase.

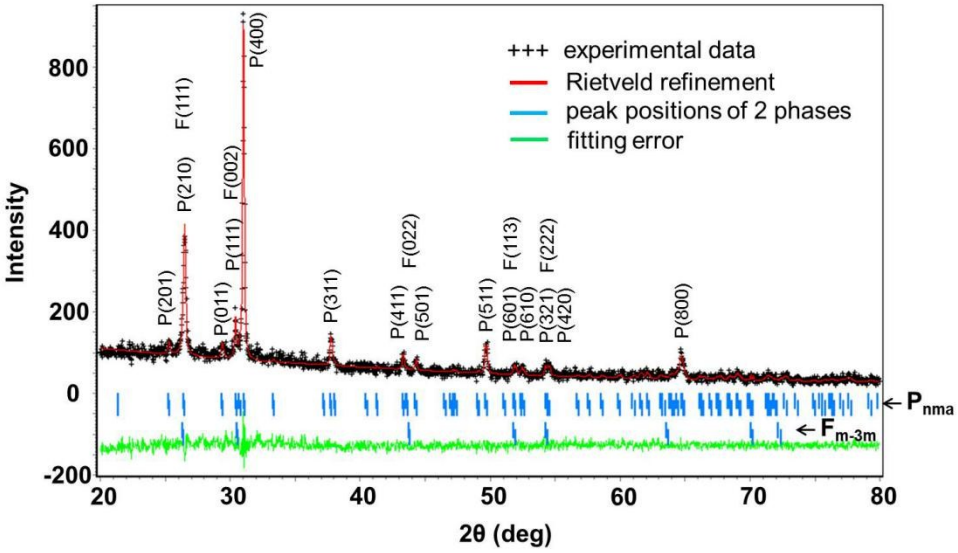

Fig. S2. The atomic structures of two phases (*Pnma*, $Fm\bar{3}m$) of SnSe. The Sn atom is in black and Se in red. The unit cells are marked in a dashed rectangle. The solid horizontal lines going through the center of some atoms are to highlight the atoms in one plane. From the phase $Fm\bar{3}m$ to *Pnma*, the size of unit cell is doubled in c direction and a relative shift of 1/2a along a direction; From $Fm\bar{3}m$ to *Pnma*, zigzag atomic line of Sn-Se-Sn along a direction becomes a pucked line.

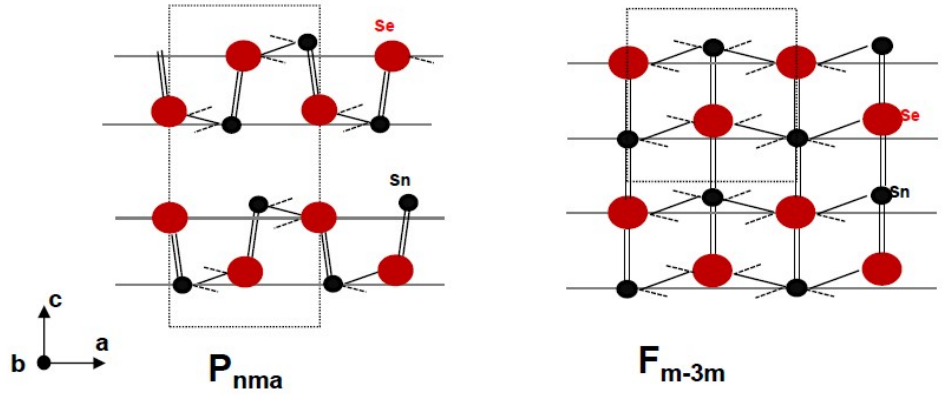

Fig. S3. Temperature dependence of specific heat for polycrystalline SnSe. We carefully carried out multiple measurements on C_p. The red circles show higher C_p than the other measurements which was used for calculating thermal conductivity.

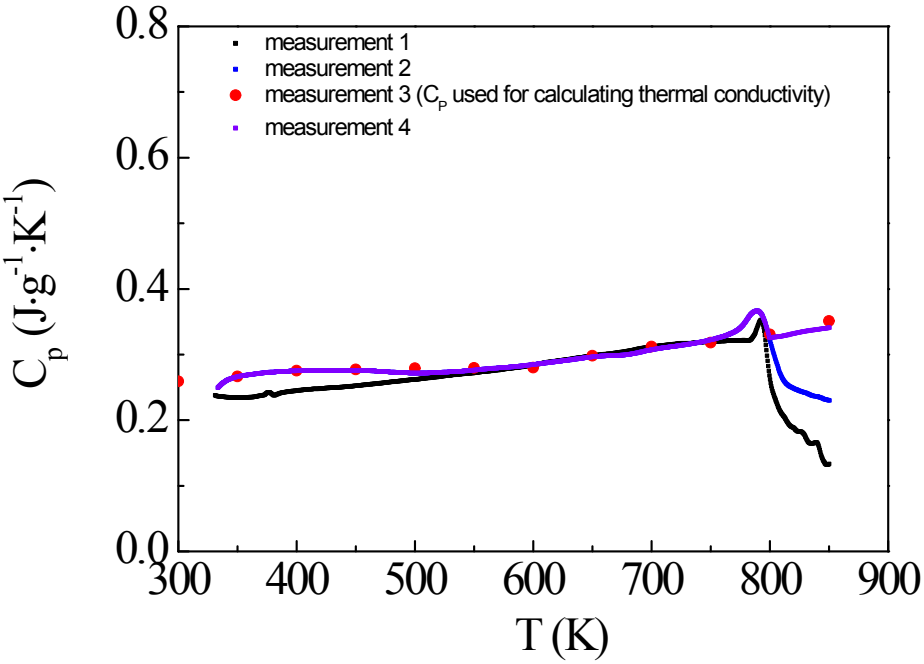

Fig. S4. (a) The electronic band structures of $Fm\bar{3}m$ phases of SnSe. Direct band gaps are found for $Fm\bar{3}m$. (b) The zoomed-in band structure near the band gap.

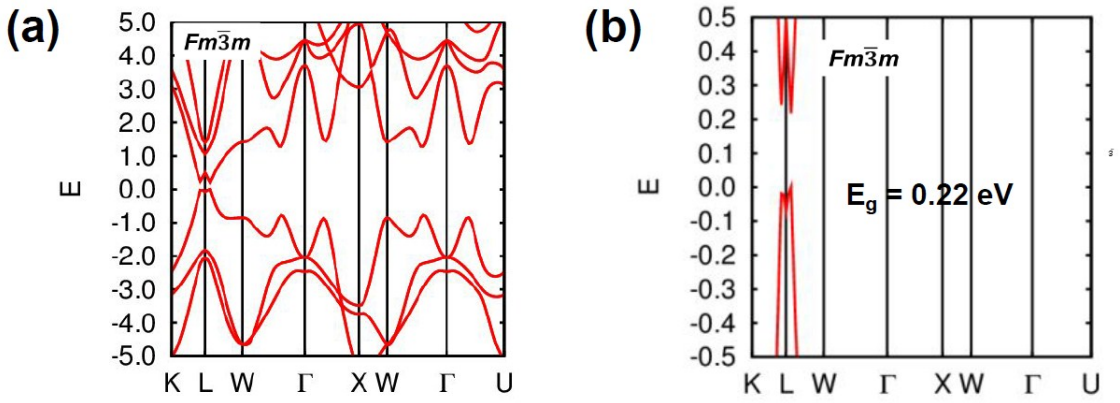

Fig. S5. Calculated thermoelectric transport properties of both *Pnma* and $Fm\bar{3}m$ phases. The dependence on temperature and carrier concentration n of (a, d) Seebeck coefficient S, (b, e) electrical conductivity, and (c, f) *PF*; (a, b, c) and (d, e, f) correspond to $Fm\bar{3}m$ and *Pnma* phases, respectively. The green dashed lines of n(T) in (c) and (f) from our calculation show the temperature-dependent hole carrier concentration of $Fm\bar{3}m$ and *Pnma*, respectively.

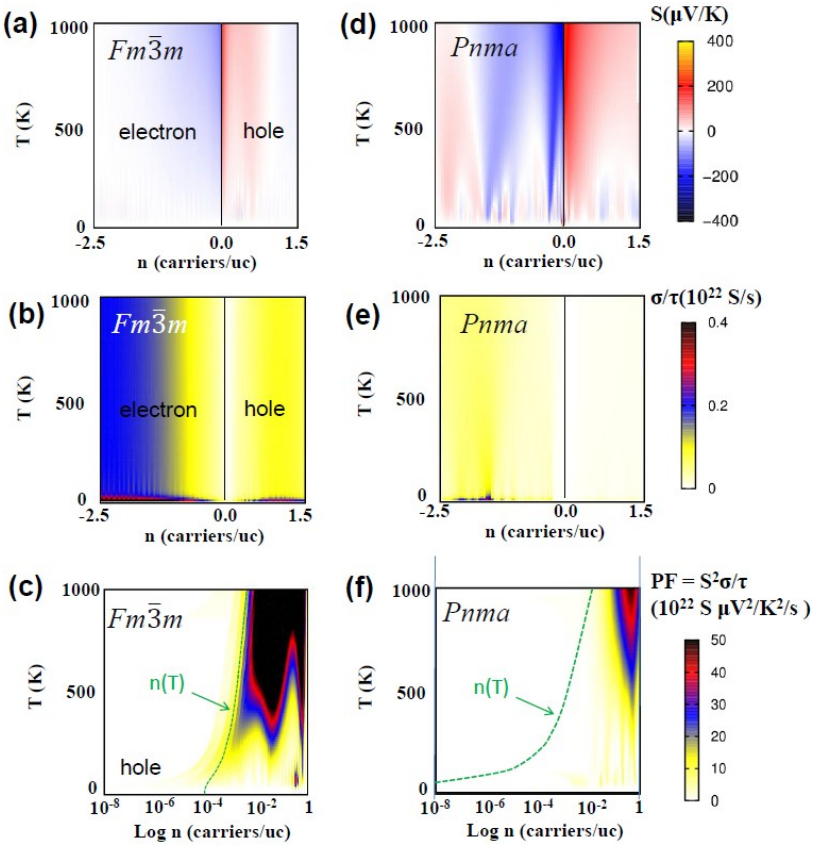

Fig. S6. Reproducibility, and temperature dependence of thermoelectric properties for three samples of polycrystalline SnSe measured parallel to the pressing direction. (a) Electrical conductivity (σ). (b) Seebeck coefficient (S). (c) Thermal conductivity (κ). (d) ZT; error bars are 15%.

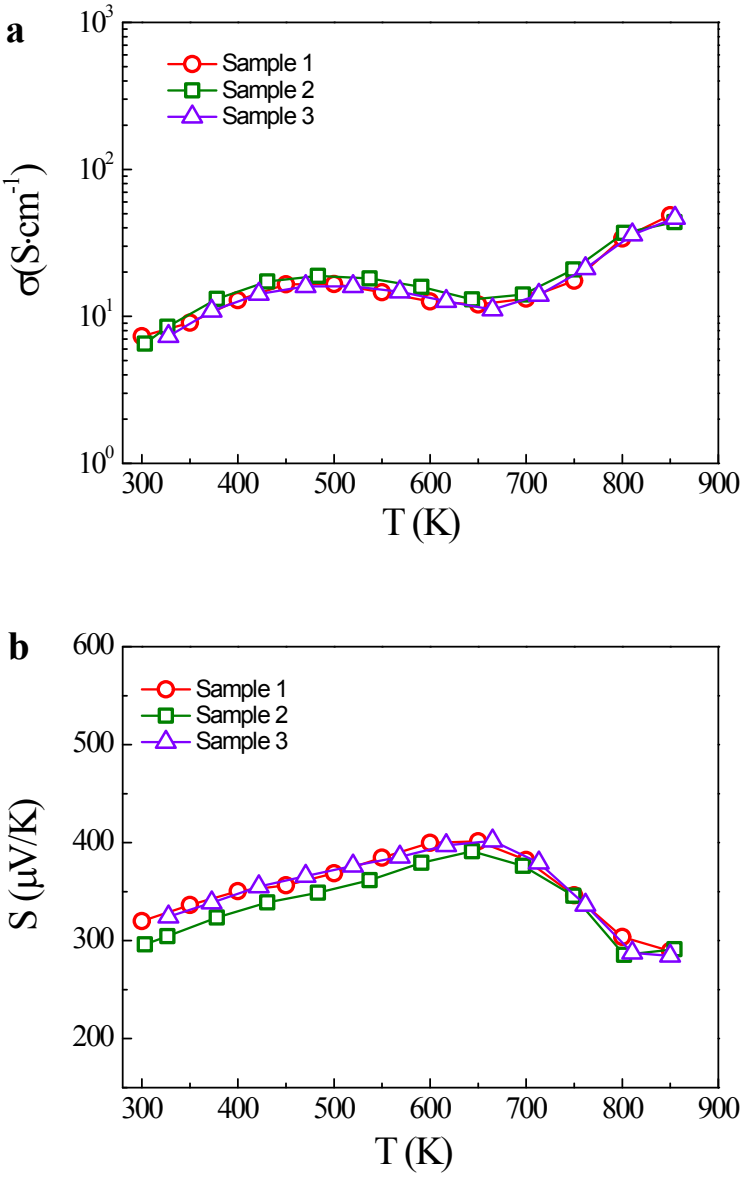

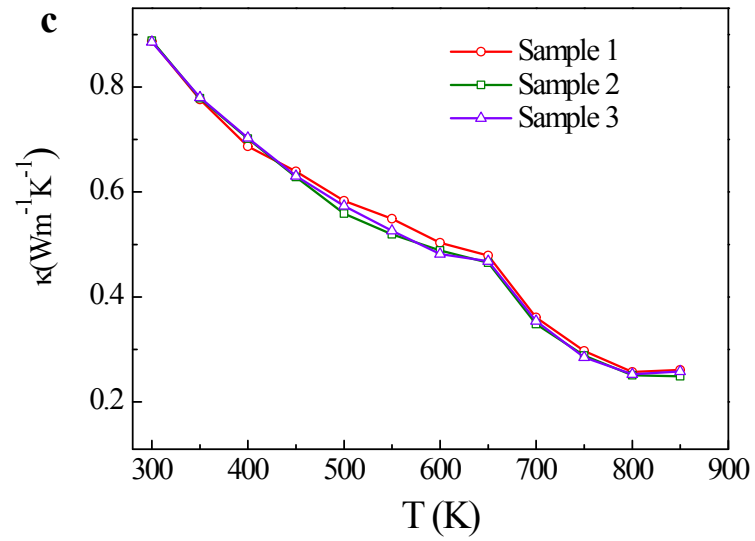
c
Sample 1
Sample 2
Sample 3
κ(Wm-1K-1)
0.2
0.4
0.6
0.8
300
400
500
600
700
800
900
T (K)

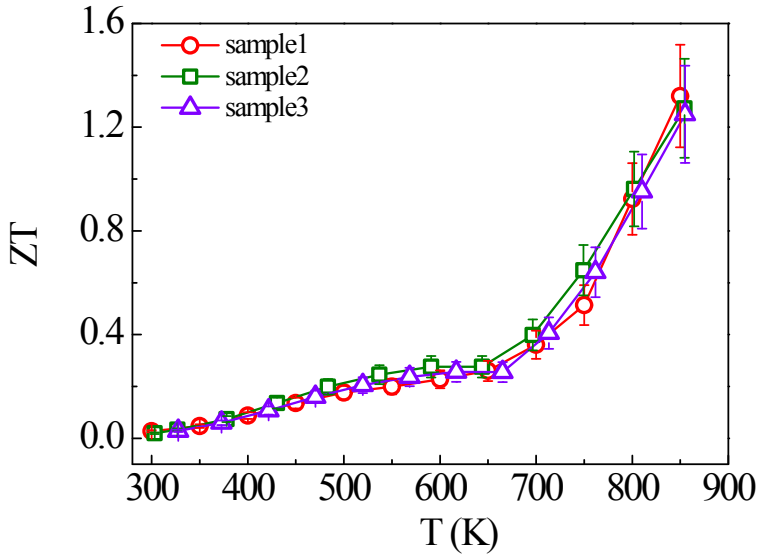
sample1
sample2
sample3
ZT
0.0
0.4
0.8
1.2
1.6
300
400
500
600
700
800
900
T (K)

References

[32] P. Blaha, K. Schwarz, G. Madsen, D. Kvasnicka, J. Luitz, *WIEN2k: An augmented plane wave plus local orbitals program for calculating crystal properties*, TU Vienna, Vienna 2011**.**

[33] J. P. Perdew, K. Burke, M. Ernzerhof, *Phys. Rev. Lett.,* 1996**, 77**, 3865.

[34] L. Zhang, D. J. Singh, *Phys. Rev. B,* 2009**, 80**, 075117.

[35] D. Parker, M. H. Du, D. J. Singh, *Phys. Rev. B,* 2011**, 83**, 245111.

[36] G. K. H. Madsen, K. Schwarz, P. Blaha, D. J. Singh, *Phys. Rev. B,* 2003**, 68**, 125212.